ACS OMEGA

Open Access

http://pubs.acs.org/journal/acsodf

Article

Molecular Dynamics Simulation of the Three-Phase Equilibrium Line of CO_2 Hydrate with OPC Water Model

Xiluo Hao, Chengfeng Li, Qingguo Meng, Jianye Sun, Li Huang, Qingtao Bu, and Congying Li*

Cite This: *ACS Omega* 2023, 8, 39847−39854

Read Online

ACCESS | Metrics & More | Article Recommendations

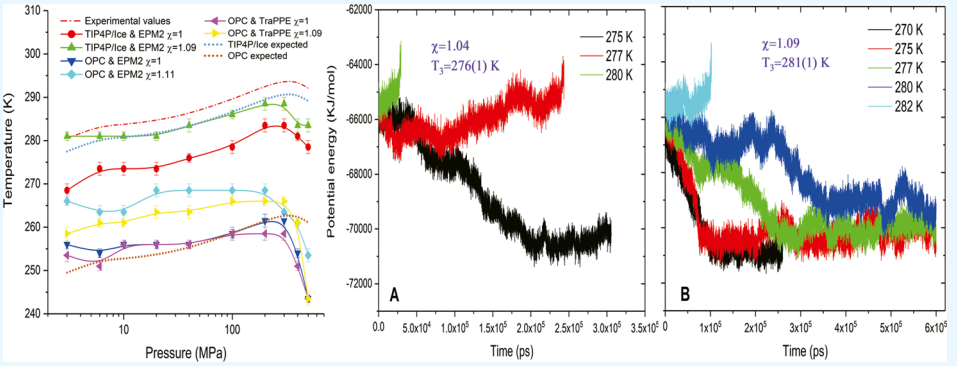

ABSTRACT: The three-phase coexistence line of the CO_2 hydrate was determined using molecular dynamics (MD) simulations. By using the classical and modified Lorentz−Berthelot (LB) parameters, the simulations were carried out at 10 different pressures from 3 to 500 MPa. For the OPC water model, simulations with the classic and the modified LB parameters both showed negative deviations from the experimental values. For the TIP4P/Ice water model, good agreement with experimental equilibrium data can be achieved when the LB parameter is adjusted based on the solubility of CO_2 in water. Our results also show that the influence of the water model on the equilibrium prediction is much larger than the CO_2 model. Current simulations indicated that the H_2O−H_2O and H_2O−CO_2 cross-interactions' parameters might contribute equally to the accurate prediction of T_3. According to our simulations, the prediction of T_3 values showed relatively higher accuracy while using the combination of TIP4P/Ice water and EPM2 CO_2 with modified LB parameter. Furthermore, varied χ values are recommended for accurate T_3 estimation over a wide pressure range. The knowledge obtained in this study will be helpful for further accurate MD simulation of the process of CO_2/CH_4 replacement.

1. INTRODUCTION

Clathrate hydrates are crystalline, nonstoichiometric ice-like compounds formed at conditions of relatively lower temperature and higher pressure.[1,2] The structure of the gas hydrate is composed of a three-dimensional network of hydrogen-bonded water molecules, giving rise to well-defined "cages" where guest molecules can reside. According to the size and number of cages within a single unit cell of the hydrate crystal, hydrate structures can be classified as sI, sII, and sH. The structure type of the hydrate is mainly determined by the size of the guest molecule.

CO_2 hydrates received increasing attention in recent years because of the global concern about greenhouse gas emission. Since the CO_2 emission caused by global warming is recognized as one of the most severe environmental threats in the future, it is urgent to find some effective methods for carbon capture and sequestration. Under such circumstances, hydrate technology became an alternative solution to both the CO_2 capture and storage processes. Specifically, carbon dioxide can be captured from flue gases in the form of hydrates,[3,4] owing to its relatively higher thermodynamic stability.[5] Moreover, methane recovery from natural methane hydrate by CO_2 replacement could provide a promising approach for simultaneous hydrocarbon retrieving and carbon sequestration.[6−9] In order to explore the potential usage of carbon dioxide hydrates, it is necessary to develop reliable methodologies for better understanding and accurate prediction of both their kinetic and equilibrium properties.

Molecular dynamics (MD) simulation has long been proved to be a useful tool for the study of clathrate hydrates.[10] It can

Received: August 16, 2023
Accepted: September 26, 2023
Published: October 10, 2023

not only provide insight into molecular phenomena but also offer a useful tool to predict the macroscopic hydrate properties when the experimental data are unavailable. In order to perform accurate simulations, the methodologies and force fields used in MD studies need validation first by comparing the MD results to reliable experimental data. The three-phase coexistence line is one of the most important parameters in hydrate studies. As methane hydrate is the most commonly found hydrate in nature, many previous MD simulations have been performed to study the phase equilibria of methane hydrate.[11−16] In these works, the performance of different H_2O models was compared, finding that the consideration of positive deviation from the ideal Lorentz−Berthelot combination rules could yield a remarkable representation of experimental coexistence results. Except for these phase equilibrium-related studies, MD simulation has been applied in a variety of research areas of methane hydrate from a molecular point of view.[10,17−28]

Compared with methane hydrate, the MD prediction of phase equilibria of CO_2 hydrate has attracted limited attention so that only a few works have been done in this research field. Sarupria and Debenedetti[29] carried out MD simulations to study the relationship between the dissociation rate and cage occupancy of carbon dioxide hydrates. Using TIP4P/2005[30] for water and TraPPE[31] for carbon dioxide, they found that the dissociation temperature is modestly related to the hydrate occupancy. As the configuration used in their study did not contain the gas phase of carbon dioxide, the dissociation temperature of the CO_2 hydrate was treated as the three-phase equilibrium temperature. They reported that the deviation between the melting point of CO_2 hydrate and the melting point of ice as predicted by TIP4P/2005[32] is about 4−8 K at 3.05 MPa, which is close to the temperature difference of the experimental hydrate T_3 and ice melting values (∼7 K). Tung et al.[33] used a three-phase configuration to simulate the growth of carbon dioxide hydrate and calculated the T_3 values at different pressure conditions. The TIP4P/Ew[34] water model and EPM2[35] CO_2 models were applied in the MD simulation, with Lennard−Jones cross-interaction parameters suggested by Sun and Duan.[36] At relatively lower pressure conditions (less than 30 MPa), their predictions agree well with the experimental values, while at higher pressure conditions (100 MPa), the deviations of T_3 become significant. Míguez et al.[37] studied the three-phase equilibria of carbon dioxide hydrate using the direct-phase coexistence method up to 500 MPa. The TIP4P/Ice[38] and TIP4*P*/2005 force fields were used for water and several different force fields were used for carbon dioxide. Their simulations showed that the evolution of the system was the same when all large cages were initially occupied (the cage occupancies range from 75 to 100%), and the influence of the water model on the T_3 prediction is obviously larger than the carbon dioxide model. At higher simulation pressure (300−500 MPa), both water models showed the retrograde behavior of the equilibrium line. For the TIP4P/Ice model, the introduction of a modified cross-interaction parameter χ = 1.13 was effective in correcting the predicted T_3 up to 200 MPa. However, T_3 was still underestimated with the modified χ value while in the pressure range of 200−400 MPa. Costandy et al.[39] also used the direct-phase coexistence methodology to predict the T_3 value of carbon dioxide hydrate in the pressure range of 20−500 MPa. The authors used the TIP4P/Ice and TIP4*P*/2005 force fields for water and the TraPPE force field for carbon dioxide. Their simulations indicated that T_3 values cannot be predicted accurately using the classic LB combination rules. The authors then modified the water−guest interaction parameters based on the solubility of carbon dioxide in water. In this case, they found that the obtained T_3 values are closely related to the melting point of ice, as predicted by the water model.

Although a variety of water models have been applied in previous MD studies on CO_2 hydrate, the water model referred to as the "optimal" point charge (OPC) water model developed by Izadi et al.[40] has not been included yet. Compared with the commonly used TIP4P/Ice water models in ice and gas hydrate simulations, the bulk properties of water (including density, self-diffusion, dielectric constant, heat capacity, etc.) reproduced by the OPC model are significantly more accurate over a wide range of temperatures. However, the melting point predicted by the OPC model exhibits a large deviation[41] when compared with the TIP4P/Ice model. Our previous study[16] has already shown the relatively good performance of the OPC model in the prediction of T_3 of methane hydrate especially at lower pressure, which encourages us to perform MD simulation to study the three-phase coexistence line of CO_2 hydrate with this water model. The present work focuses on the prediction of the phase equilibria of carbon dioxide hydrate with an emphasis on the role of water−guest interactions in the determination of the three-phase coexistence temperature. To this purpose, we follow the direct-phase coexistence methodology that was successfully used in our previous study of methane hydrates. In line with the work of Miguez et al.,[37] we test two different CO_2 force fields, namely, TraPPE and EPM2, in combination with the OPC force field for water. Also, the combination of the TIP4P/Ice water model and the EMP2 CO_2 model is included for comparison.

2. METHODOLOGY

The direct-phase coexistence method is used in the current study to determine the coexistence temperature in the CO_2−water−hydrate system. The system configuration of this study consists of a CO_2 hydrate slab, a CO_2 slab, and two liquid water slabs. The CO_2 gas slab is inserted into two water slabs to generate a hydrate−water−CO_2−water arrangement. A buffer distance of 0.1 nm is assigned between each slab to avoid bad contacts while processing energy minimization.

The hydrate slab is composed of 2 × 2 × 2 cubic unit cells (368 water molecules and 64 CO_2 molecules). Each hydrate unit cell is built as follows: positions of the water oxygen atoms are obtained from X-ray crystallography,[42] and the water hydrogen atoms are inserted by adjusting the orientations to obey the Bernal−Fowler rule and minimize the potential energy and net unit cell dipole moment.[43] CO_2 molecules are assumed to fully occupy the water polyhedral cages constituted by the water hydrogen bond network and situate at the cage center. Each water slab contains 368 water molecules, and the CO_2 gas slab contains 256 CO_2 molecules to avoid the generation of a gas bubble during hydrate formation. Totally 1104 water molecules and 320 CO_2 molecules are present in the initial simulation box with initial dimensions of 2.5 × 2.5 × 9.6 nm^3. A snapshot of the initial configuration of the simulation box before pre-equilibrium is shown in Figure 1. The TIP4P/Ice and the OPC water models are adopted for water molecules, while the TraPPE and EMP2 models are used for CO_2. A total of six sets of simulations were conducted (combination of OPC with TraPPE or EPM2 and TIP4P/Ice

https://doi.org/10.1021/acsomega.3c05673
ACS Omega 2023, 8, 39847−39854

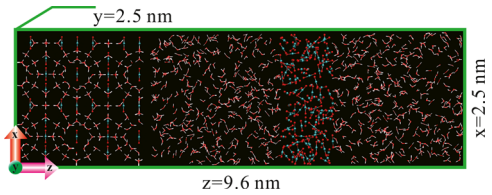

Figure 1. Initial configuration of the simulation system for the direct coexistence method before equilibrium. The red and white lines represent water molecules, and the cyan and red spheres represent CO_2 molecules.

with EPM2), of which three used the classical LB combination rules to determine the water−gas interaction, and the other three used a modified factor (χ) to correct the LB cross-interaction energy parameter, as shown in the following equation:

$$\varepsilon_{CO_2-H_2O} = \chi\sqrt{\varepsilon_{CO_2-CO_2}\varepsilon_{H_2O-H_2O}} \quad (1)$$

The χ value is determined based on the solubility of CO_2 in water. To calculate the solubility dependence on χ, the simulation box is built with 2000 water molecules and 500 CO_2 molecules. The pressure and temperature conditions to calculate the solubility of CO_2 are 40 MPa and 286 K. After a 500 ps NVT temperature equilibration, NPT simulations with the duration of 200 ns were performed while the χ value varied from 1 to 1.18 with an increment of 0.02. Then, the mole fraction of carbon dioxide in the water slab away from the interface was calculated after the system reached its equilibrium state (after 50 ns). In order to reduce the statistical uncertainty, totally 100 measurements of carbon dioxide solubility in water for each χ value were used for solubility estimation. The atomic charges, Lennard−Jones parameters, and interatomic distances of the models used in this study are summarized in Table 1.

Molecular simulations are performed using the Gromacs package version 5.1.5.[44,45] Newton's equation of motion is integrated using the leapfrog algorithm with a 2 fs time step. Periodic boundary conditions are introduced in all three dimensions. The long-range electrostatic interactions[46] are handled with the particle-mesh Ewald summation method and the cutoff distance is adjusted to 1.0 nm. The van der Waals interactions are calculated using the Lennard−Jones potential with a cutoff radius of 1.0 nm. Velocity-rescale thermostat algorithm is adopted for temperature control, and the time constant is 0.5 ps. The pressure of the simulation systems is controlled by semi-isotropic Parrinello−Rahman barostat (for hydrate formation) and isotropic Parrinello−Rahman barostat (for solubility calculation), respectively, with a 1 ps relaxation time.

For hydrate formation simulations, energy minimization is first performed with the steepest descent algorithm to relax the liquid water at the hydrate surface. Then, a 500 ps simulation run under the NVT ensemble is carried out for temperature equilibrium and followed by the NPT production simulation. Totally 10 equilibrate pressure conditions are selected, namely, 3, 6, 10, 20, 40, 100, 200, 300, 400, and 500 MPa. The equilibrium temperature varies from 240 to 295 K for each independent simulation run. Each simulation will continue until complete formation or dissociation of CO_2 hydrate is achieved.

3. RESULTS AND DISCUSSION

3.1. Equilibrium Conditions with Classical LB Combination Rule. The combination of the OPC water with EPM2 or TraPPE carbon dioxide was examined first using classical LB combining rules. Meanwhile, the use of TIP4P/Ice and EPM2 was also included for comparison. The T_3 at 10 different pressure conditions were calculated. As shown in Figure 2, two

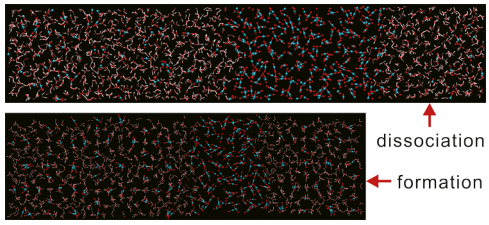

Figure 2. Snapshots of the simulation box at 40 MPa, using the TIP4P/Ice model for water, the EPM2 model for CO_2, and the modified LB combining rules (T_3 = 283.5 K), and the two final states at 282 and 285 K correspond to complete hydrate dissociation and formation, respectively. The water molecules are represented by the red and white lines, while the carbon dioxide molecules are represented by the cyan (carbon) and red (oxygen) spheres.

Table 1. Potential Parameters of TIP4P/Ice (Water), OPC (Water), EPM2 (CO_2), and TraPPE (CO_2) Models[a]

force field	atom	σ_{LJ} (Å)	ϵ_{LJ} (kJ/mol)	q (e)	geometry
TIP4P/Ice					
	O	3.1668	0.88217	0	d_{OH} = 0.9572 Å
	H	0	0	0.5897	d_{OM} = 0.1577 Å
	M	0	0	−1.1794	H−O−H = 104.52°
OPC					
	O	3.16655	0.89036	0	d_{OH} = 0.8724 Å
	H	0	0	0.6791	d_{OM} = 0.1594 Å
	M	0	0	−1.3582	H−O−H = 103.6°
EMP2					
	C	2.757	0.23388	0.6512	d_{OC} = 1.149 Å
	O	3.033	0.66937	−0.3256	O−C−O = 180°
TraPPE					
	C	2.80	0.22459	0.70	d_{OC} = 1.16 Å
	O	3.05	0.65712	−0.35	O−C−O = 180°

[a]The geometry, partial charges (q), and the L−J parameters σ and ε are given for all of the atoms and the negative charge site of the water model (M).

https://doi.org/10.1021/acsomega.3c05673
ACS Omega 2023, 8, 39847−39854

indicative snapshots of the simulations performed at 40 MPa represented the final states of the system: complete CO_2 hydrate dissociation and formation occurred at 285 and 282 K, respectively. The representative evolution of the potential energy of the simulation system at different temperatures is presented in Figure 3. The decrease in the total potential

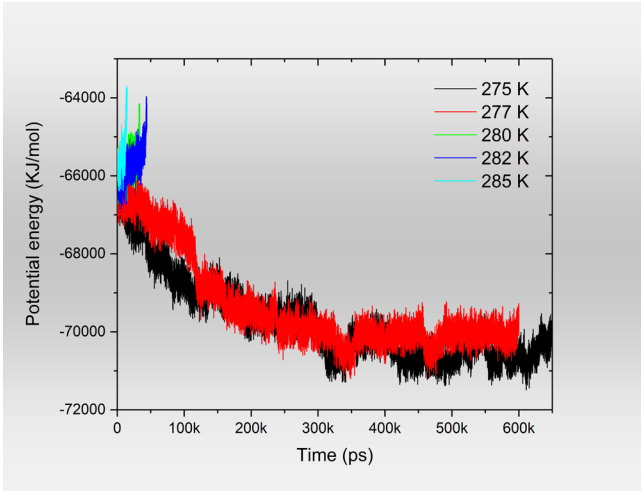

Figure 3. Evolution of the potential energy as a function of time for the NPT runs for the TIP4P/Ice and EPM2 models at 100 MPa.

energy indicates the growth of CO_2 hydrate, while the increase indicates hydrate dissociation. Since we only conducted one single simulation at each temperature−pressure condition, the value of T_3 is assigned as the arithmetic average of the lowest hydrate dissociation temperature and the highest hydrate formation temperature. Take the temperature scan shown in Figure 3 as an example. The T_3 at 100 MPa would be estimated as 278.5 K.

The calculated T_3 values for the three sets of simulations are given in Table 2 and are presented in Figure 4. For the pressures examined, the use of the OPC water model with the classical LB rules generates large deviations of T_3, which are approximately 25−50 K for both EMP2 and TraPPE CO_2 models. Our results indicate that the usage of different CO_2 models makes only a small difference in T_3 prediction, which agrees well with the conclusion made by Míguez et al.[37] Comparably, simulations using TIP4P/Ice water with LB rules

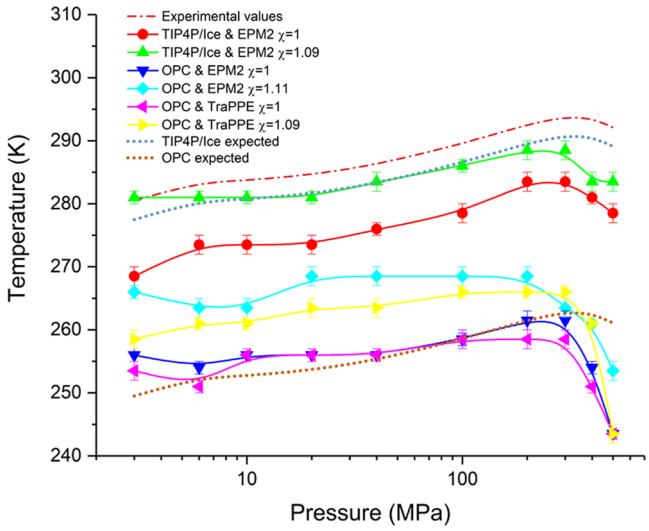

Figure 4. Experimental (red dash-dot line) and predicted values of T_3 for carbon dioxide hydrates from this work. The blue and brown dashed lines represent the expected values of T_3 for the TIP4P/Ice (experimental values − 3 K) and the OPC (experimental values − 31 K) force fields, respectively. Experimental values were obtained from ref 2.

result in a much smaller T_3 deviation of only 10−14 K. Both TIP4P/Ice and the OPC models cannot reproduce experimental T_3 of CO_2 hydrate combined with a CO_2 model using ideal Lorentz−Berthelot cross-combining parameters. However, the equilibrium curve of each simulation set exhibits reentrant behavior at high-pressure conditions, and the shape of equilibrium lines are similar with that of the experimental line, especially for TIP4P/Ice model.

3.2. Solubility-Based χ-value Calculation. The above results indicated that both the OPC and the TIP4P/Ice water models cannot reproduce the experimental T_3 of the CO_2 hydrate using ideal LB combination parameters. Previous studies on the nucleation of CO_2 hydrate have revealed the importance of the modification of LB parameters in MD simulation to obtain proper CO_2 concentration and to trigger nucleation.[47] Thus, a proper modification is needed for T_3 prediction of the CO_2 hydrate using MD simulation. Míguez et al.[37] and Costandy et al.[39] used different approaches to modify the interaction between molecules to correct the deviation between the predicted and experimental T_3 values of gas

Table 2. Experimental and Calculated T_3 of the Six Sets of Simulations Using Ideal (χ = 1.00) and Modified LB Combining Rules

	T_3 (K)						
		TIP4P/Ice and EPM2		OPC and EPM2		OPC and TraPPE	
pressure (MPa)	experimental	χ = 1	χ = 1.09	χ = 1	χ = 1.11	χ = 1	χ = 1.09
3	280.5	268.5(1.5)	281(1)	256(1)	266(1)	253.5(1.5)	258.5(1.5)
6	283.4	273.5(1.5)	281(1)	254(1)	263.5(1.5)	251(1)	261(1)
10	283.7	273.5(1.5)	281(1)	256(1)	263.5(1.5)	256(1)	261(1)
20	284.6	273.5(1.5)	281(1)	256(1)	268.5(1.5)	256(1)	263.5(1.5)
40	286.2	276(1)	283.5(1.5)	256(1)	268.5(1.5)	256(1)	263.5(1.5)
100	289.5	278.5(1.5)	286(1)	258.5(1)	268.5(1.5)	258.5(1.5)	266(1)
200	292.6	283.5(1.5)	288.5(1.5)	261.5(1.5)	268.5(1.5)	258.5(1.5)	266(1)
300	293.8	283.5(1.5)	288.5(1.5)	261.5(1.5)	263.5(1.5)	258.5(1.5)	266(1)
400	293.6	281(1)	283.5(1.5)	254(1)	261(1)	251(1)	261(1)
500	292.1	278.5(1.5)	283.5(1.5)	243.5(1.5)	253.5(1.5)	243.5(1.5)	243.5(1.5)

https://doi.org/10.1021/acsomega.3c05673
ACS Omega 2023, 8, 39847−39854

hydrate. Míguez et al.[37] performed simulations at the same temperature and pressure conditions and tested different cross-interaction energy parameter values, until a good consistency of predicted T_3 and experimental T_3 was achieved (the corresponding χ value is 1.13). Differently, Costandy et al.[39] used the solubility of CO_2 in water to modify the cross-interaction parameter. They tested the deviation between the predicted solubility and the values reported by Duan et al.[48] at the same P−T conditions and found that the deviation could be minimized when the modification parameter χ value was 1.08. Using this modified LB parameter, Costandy et al.[39] confirmed that the deviation between predicted and experimental T_3 of CO_2 hydrate was equal to the bias of the water model in predicting the melting temperature of ice.

A similar methodology as described in Costandy et al.[39] was applied in our work to modify the cross-parameter between water and carbon dioxide. The results of the modification simulation are presented in Figure 5. It is shown that the

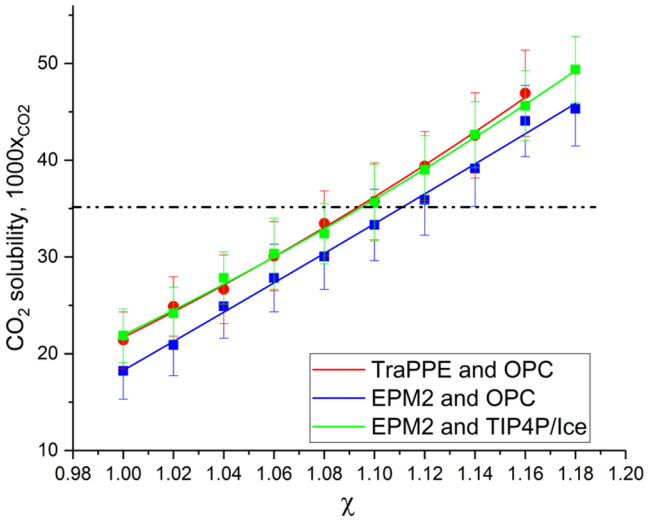

Figure 5. Dependence of the solubility of CO_2 in water on the modification factor of the LB cross-interaction energy parameter for the three sets of simulations with different molecule models. The dashed line shows the solubility of CO_2 obtained by Duan's equation[48] at 40 MPa and 286 K.

solubility of CO_2 in water can be predicted accurately with χ value of 1.09 for the combination of TIP4P/Ice and EPM2 models; while for the OPC model, the χ values are 1.11 and 1.09 for EMP2 and TraPPE CO_2 models, respectively. As described in Section 2, these χ values were all obtained at 40 MPa and 286 K. In order to validate the suitability of the χ values in the wide range of P−T conditions performed in our study, the CO_2 solubility around hydrate equilibrium points from 3 to 200 MPa was re-examined, and the results are shown in Figure 6. At a pressure range from 6 to 100 MPa, the calculated solubilities by three sets of simulation are in good agreement with the values obtained using Duan's equation[46] along the three-phase equilibrium line. However, the CO_2 solubility is overestimated at lower pressure (3 MPa) and underestimated at higher pressure (200 MPa) when compared with the experimental values. Note that the predicted CO_2 solubility data above 200 MPa were not provided. One reason is that Duan's equation does not support solubility calculations above 200 MPa for comparison. Another reason is that we observed the generation and collapse of a CO_2 gas bubble in

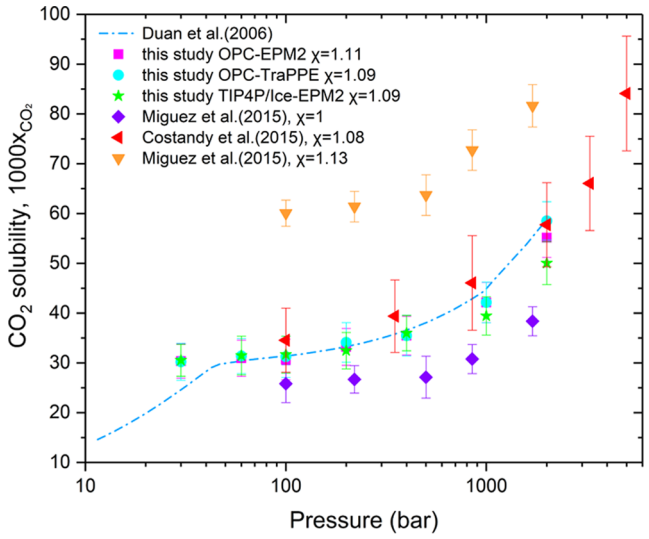

Figure 6. CO_2 Solubility in water as a function of pressure under hydrate equilibrium conditions. The dashed cyan line is the data calculated based on the work of Duan et al.[48] Purple diamonds and brown down-triangles are results from the work of Míguez et al.[37] with χ = 1 and χ = 1.13, respectively. Red triangles are results from the work of Costandy et al.[39] with χ = 1.08 using TIP4P/Ice−TraPPE combination.

our simulation box when the pressure exceeds 200 MPa, so the estimation of the CO_2 solubility becomes inconvincible.

3.3. Equilibrium Conditions with Corrected Cross-Parameters. Using the above modified interaction parameters, all of the simulation runs were performed one more time to calculate the T_3 values of carbon dioxide hydrate. The results are shown in Table 2 and are also presented in Figure 4. It is quite clear that the correction of the CO_2 solubility significantly affected the predicted T_3 values. The deviations between the predicted T_3 and the experimental T_3 range from 0.5 to −10, −20 to −32, and −22 to −49 K for TIP4P/Ice and EPM2, OPC and EPM2, and the corresponding OPC and TraPPE force fields, respectively.

For the TIP4P/Ice model, the deviation of T_3 from the experimental values was approximately −3 K in the pressure range (6 to 100 MPa) that the CO_2 solubility in water can be accurately modified. This value is equal to the deviation of the predicted melting point of ice (−3 K) as determined by TIP4P/Ice. The result strongly supports that the accuracy of the prediction of T_3 by TIP4P/Ice can be improved on the grounds of an accurate description of the water−guest interactions based on the gas solubility in water. For the OPC model, the deviation of the predicted T_3 from the experimental values is significantly smaller than the difference between the estimated and experimental values of Ice Ih melting temperature (~31 K at 0.1 MPa) except for the simulations performed at high pressure (400 and 500 MPa). As depicted in Figure 4, the predicted T_3 values with the OPC and ideal LB parameters appear to be closer to the expected values (T_3, experimental − 31 K) within a larger pressure range. In other words, the OPC model does not agree with previous findings[39] that the deviation of T_3 is dictated by the deviation of the predicted melting temperature of ice, which is consistent with our previous findings on methane hydrate.[16] We speculated that the predicted hydrate T_3 value is probably correlated with not only the ice point of the specific water model as reported by Costandy et al.[39] but also the accuracy of

https://doi.org/10.1021/acsomega.3c05673
ACS Omega 2023, 8, 39847−39854

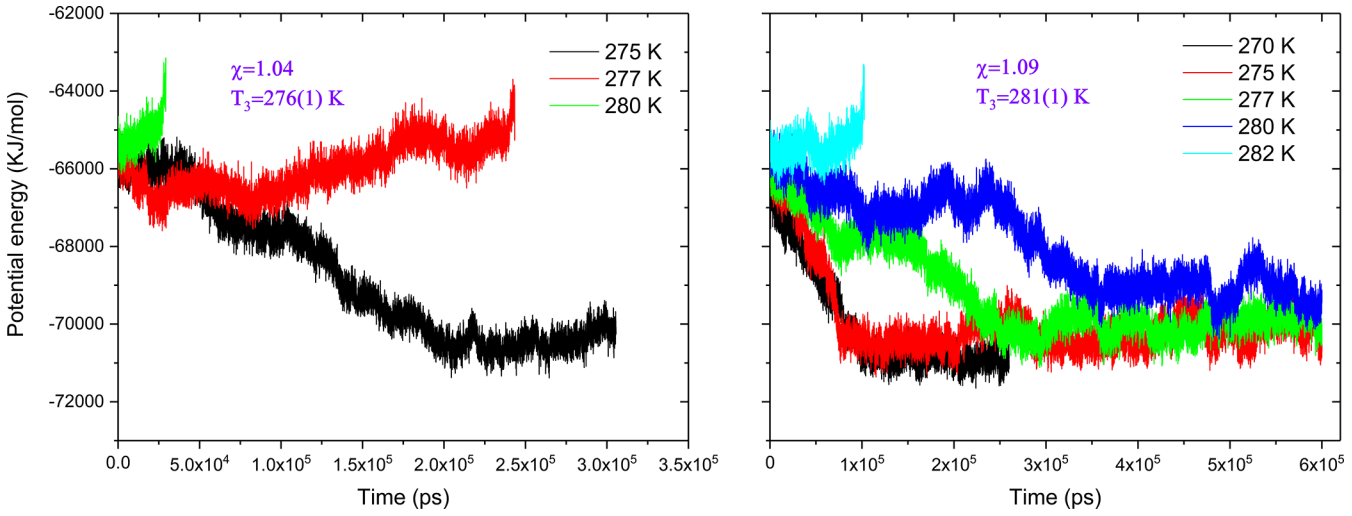

Figure 7. Evolution of the potential energy as a function of time for the NPT simulations at 3 MPa with two different χ values.

the reproduced bulk properties of water. The influence of the latter is comparable to the amendment of the H_2O-CO_2 interaction based on the CO_2 solubility.

It is worth noting that at lower (3 MPa) and higher (over 200 MPa) pressure conditions, the T_3 deviation from experimental values becomes larger. This trend is consistent with the predicted CO_2 solubility. To further verify the influence of CO_2 solubility, we recalculated the χ value for the combination of TIP4P/Ice and EMP2 models at 3 MPa. The result showed that the CO_2 solubility can be correctly predicted with an LB modification parameter of χ = 1.04. Using this parameter, the equilibrium temperature of CO_2 hydrate at 3 MPa was calculated to be 276 ± 1 K (Figure 7), which is about 3 K lower than the experimental value. The results strongly confirmed the importance of CO_2 solubility in accurate T_3 prediction. Unfortunately, there are no convincing CO_2 solubility data at higher pressure (over 200 MPa). Therefore, the determination of χ values at higher pressure conditions becomes unavailable. However, we could also note the trend of underestimation of CO_2 solubility while the pressure goes higher, which might imply a larger χ (over 1.09) is needed for accurate T_3 prediction. Our simulations indicated that a fixed modification parameter χ is not enough for the accurate prediction of carbon dioxide solubility under all pressure conditions. Thus, a varied χ is needed to correctly describe the three-phase equilibrium line within the large pressure range. Our results are somewhat different from Costandy's findings which used only one fixed χ to reproduce the experimental T_3 in the pressure range from 20 to 500 MPa. One possible reason might be the accuracy of the TraPPE CO_2 model in solubility estimation at higher pressure. As shown in Figure 6, the CO_2 solubility predicted by the combination of TraPPE and TIP4P/Ice models (red triangles) seems to have smaller deviations compared with our calculations. Moreover, simulations conducted at a pressure lower than 20 MPa were not included in Constandy's work, under which conditions the CO_2 solubility might be overestimated. In light of this, we conducted the solubility and T_3 prediction at 3 MPa using exactly the same parameters as reported in Constandy et al.[39] The obtained CO_2 solubility was basically consistent with those values we previously obtained using different models under the same condition. Moreover, the predicted T_3 value at this specific pressure was ~279 K. The deviation between the predicted T_3 and experimental value was slightly smaller than the reported bias (−2.2 to −3.9 K). The above simulations implied that the usage of an χ value smaller than 1.08 might generate a more precise prediction of both the CO_2 solubility and T_3 values while using TIP4P/Ice and TraPPE models.

4. CONCLUSIONS

In this work, the direct coexistence method was used to calculate the three-phase coexistence line of the CO_2 hydrate. Totally, six sets of simulations were conducted to calculate the coexistence temperatures T_3 for 10 pressure conditions ranging from 3 to 500 MPa. For simulations using ideal LB combination parameters, all three sets of simulations showed significantly underestimation of T_3 when compared with the experimental values. Meanwhile, the re-entrant behavior of the equilibrium curve can be observed. The three-phase equilibrium line obtained by the combination of TIP4P/Ice and EPM2 models almost strictly obeys the experimental trend with a temperature shift of about 10−14 K. This discrepancy is speculated to be aroused by the combined underestimation of CO_2 solubility in water and ice melting point. Based on the solubility of CO_2 in water at 40 MPa and 286 K, the cross-interaction parameters χ were calculated to be 1.09, 1.11, and 1.09 for the combination of TIP4P/Ice and EPM2, OPC and EMP2, and OPC and TraPPE models, respectively. Using the above modified LB parameters, the deviations between the corresponding T_3 values and experimental values all become smaller. For TIP4P/Ice and EPM2 models at a pressure range from 20 to 200 MPa, the deviation is almost equal to the difference in the predicted melting point of ice from the respective experimental value. On the contrary, the simulations using the OPC water model and ideal LB parameters agree well with the idea that the deviation is correlated with the difference in the prediction of the melting point of ice from the respective experimental value. Considering the relatively higher ability of the OPC model in reproducing bulk properties of water, we speculated that the H_2O-H_2O and H_2O-CO_2 cross-interactions' parameters might contribute equally to the prediction of T_3 value.

Additionally, the solubility of CO_2 in water was overestimated at a lower pressure and underestimated at a higher pressure, indicating that a fixed χ value may not be suitable for the T_3 prediction over a large pressure range. Based on our

https://doi.org/10.1021/acsomega.3c05673
ACS Omega 2023, 8, 39847−39854

simulations, we suggested a small χ value for the prediction of CO_2 hydrate T_3 at lower pressures (lower than 10 MPa), specifically 1.04 for TIP4P/Ice and EPM2 models at 3 MPa. At high-pressure conditions, for example, over 200 MPa, the estimation of both T_3 and CO_2 solubility implied that a relatively larger χ value (>1.09) is needed for accurate T_3 prediction. However, the lack of CO_2 solubility data prevents us from giving the exact χ value.

Finally, the large deviation in the T_3 prediction of the OPC model means that this model may not be suitable for the MD simulation of the CO_2 hydrate involving phase equilibrium conditions. The suggested models for CO_2 hydrate simulation are TIP4P/Ice and TraPPE with proper LB parameters, which can predict the CO_2 solubility in water accurately at corresponding P−T conditions.

AUTHOR INFORMATION

Corresponding Author

Congying Li − *Center of Deep Sea Research, Institute of Oceanology, Chinese Academy of Sciences, Qingdao 266071, China; Laboratory for Marine Mineral Resources, Laoshan Laboratory, Qingdao 266071, China*; Email: licongying@qdio.ac.cn

Authors

Xiluo Hao − *Key Laboratory of Gas Hydrate, Ministry of Natural Resources, Qingdao Institute of Marine Geology, Qingdao 266071, China; Laboratory for Marine Mineral Resources, Laoshan Laboratory, Qingdao 266071, China*; orcid.org/0000-0001-8202-2980

Chengfeng Li − *Key Laboratory of Gas Hydrate, Ministry of Natural Resources, Qingdao Institute of Marine Geology, Qingdao 266071, China; Laboratory for Marine Mineral Resources, Laoshan Laboratory, Qingdao 266071, China*

Qingguo Meng − *Key Laboratory of Gas Hydrate, Ministry of Natural Resources, Qingdao Institute of Marine Geology, Qingdao 266071, China; Laboratory for Marine Mineral Resources, Laoshan Laboratory, Qingdao 266071, China*

Jianye Sun − *Key Laboratory of Gas Hydrate, Ministry of Natural Resources, Qingdao Institute of Marine Geology, Qingdao 266071, China; Laboratory for Marine Mineral Resources, Laoshan Laboratory, Qingdao 266071, China*

Li Huang − *Key Laboratory of Gas Hydrate, Ministry of Natural Resources, Qingdao Institute of Marine Geology, Qingdao 266071, China; Laboratory for Marine Mineral Resources, Laoshan Laboratory, Qingdao 266071, China*

Qingtao Bu − *Key Laboratory of Gas Hydrate, Ministry of Natural Resources, Qingdao Institute of Marine Geology, Qingdao 266071, China; Laboratory for Marine Mineral Resources, Laoshan Laboratory, Qingdao 266071, China*

Complete contact information is available at: https://pubs.acs.org/10.1021/acsomega.3c05673

Notes

The authors declare no competing financial interest.

ACKNOWLEDGMENTS

The authors are grateful to the Center for High Performance Computing and System Simulation, Laoshan Laboratory, for resource allocation. This study was financially supported by the National Natural Science Foundation of China (Grant Nos. 41976205 and 41906189), the Youth Innovation Promotion Association of the Chinese Academy of Sciences (Grant No. 2020212), the Shandong Provincial Natural Science Foundation (ZR2022MD008), and the Marine Geological Survey Program (DD20221704).

REFERENCES

(1) Sloan, E. D. Fundamental principles and applications of natural gas hydrates. *Nature* **2003**, *426* (6964), 353−359.

(2) Sloan, E. D.; Koh, C. A. *Clathrate Hydrate of Natural Gases*, 3rd ed.; CRC Press, Taylor & Francis Group, 2008.

(3) Adeyemo, A.; Kumar, R.; Linga, P.; Ripmeester, J.; Englezos, P. Capture of carbon dioxide from flue or fuel gas mixtures by clathrate crystallization in a silica gel column. *Int. J. Greenhouse Gas Control* **2010**, *4* (3), 478−485.

(4) Kvamme, B.; Tanaka, H. Thermodynamic Stability of Hydrates for Ethane, Ethylene, and Carbon Dioxide. *J. Phys. Chem. A* **1995**, *99* (18), 7114−7119.

(5) Kang, S.-P.; Lee, H. Recovery of CO_2 from Flue Gas Using Gas Hydrate: Thermodynamic Verification through Phase Equilibrium Measurements. *Environ. Sci. Technol.* **2000**, *34* (20), 4397−4400.

(6) Komatsu, H.; Ota, M.; Smith, R. L.; Inomata, H. Review of CO_2−CH_4 clathrate hydrate replacement reaction laboratory studies − Properties and kinetics. *J. Taiwan Inst. Chem. Eng.* **2013**, *44* (4), 517−537.

(7) Lee, H.; Seo, Y.; Seo, Y.-T.; Moudrakovski, I. L.; Ripmeester, J. A. Recovering Methane from Solid Methane Hydrate with Carbon Dioxide. *Angew. Chem., Int. Ed.* **2003**, *42* (41), 5048−5051.

(8) Ohgaki, K.; Takano, K.; Sangawa, H.; Matsubara, T.; Nakano, S. Methane Exploitation by Carbon Dioxide from Gas Hydrates—Phase Equilibria for CO_2-CH_4 Mixed Hydrate System. *J. Chem. Eng. Jpn.* **1996**, *29* (3), 478−483, DOI: 10.1252/jcej.29.478.

(9) Park, Y.; Kim, D.-Y.; Lee, J.-W.; Huh, D.-G.; Park, K.-P.; Lee, J.; Lee, H. Sequestering carbon dioxide into complex structures of naturally occurring gas hydrates. *Proc. Natl. Acad. Sci. U.S.A.* **2006**, *103* (34), 12690−12694.

(10) English, N. J.; MacElroy, J. M. D. Theoretical studies of the kinetics of methane hydrate crystallization in external electromagnetic fields. *J. Chem. Phys.* **2004**, *120* (21), 10247−10256.

(11) Conde, M. M.; Vega, C. Determining the three-phase coexistence line in methane hydrates using computer simulations. *J. Chem. Phys.* **2010**, *133* (6), No. 064507.

(12) Conde, M. M.; Vega, C. Note: A simple correlation to locate the three phase coexistence line in methane-hydrate simulations. *J. Chem. Phys.* **2013**, *138* (5), No. 056101.

(13) Michalis, V. K.; Costandy, J.; Tsimpanogiannis, I. N.; Stubos, A. K.; Economou, I. G. Prediction of the phase equilibria of methane hydrates using the direct phase coexistence methodology. *J. Chem. Phys.* **2015**, *142* (4), No. 044501.

(14) Tung, Y.-T.; Chen, L.-J.; Chen, Y.-P.; Lin, S.-T. The Growth of Structure I Methane Hydrate from Molecular Dynamics Simulations. *J. Phys. Chem. B* **2010**, *114* (33), 10804−10813.

(15) Smirnov, G. S.; Stegailov, V. V. Melting and superheating of sI methane hydrate: Molecular dynamics study. *J. Chem. Phys.* **2012**, *136* (4), No. 044523.

(16) Hao, X. L.; Li, C. F.; Liu, C. L.; Meng, Q. G.; Sun, J. Y. The performance of OPC water model in prediction of the phase equilibria of methane hydrate. *J. Chem. Phys.* **2022**, *157*, No. 014504.

(17) Chialvo, A. A.; Houssa, M.; Cummings, P. T. Molecular Dynamics Study of the Structure and Thermophysical Properties of Model sI Clathrate Hydrates. *J. Phys. Chem. B* **2002**, *106* (2), 442−451.

(18) Fang, B.; Ning, F.; Ou, W.; Wang, D.; Zhang, Z.; Yu, Y.; Lu, H.; Wu, J.; Vlugt, T. J. H. The dynamic behavior of gas hydrate dissociation by heating in tight sandy reservoirs: A molecular dynamics simulation study. *Fuel* **2019**, *258*, No. 116106.

(19) Guo, G.-J.; Zhang, Y.-G.; Li, M.; Wu, C.-H. Can the dodecahedral water cluster naturally form in methane aqueous solutions? A molecular dynamics study on the hydrate nucleation mechanisms. *J. Chem. Phys.* **2008**, *128* (19), No. 194504.

(20) Jacobson, L. C.; Hujo, W.; Molinero, V. Amorphous Precursors in the Nucleation of Clathrate Hydrates. *J. Am. Chem. Soc.* **2010**, *132* (33), 11806−11811.
(21) Jiang, H.; Myshakin, E. M.; Jordan, K. D.; Warzinski, R. P. Molecular Dynamics Simulations of the Thermal Conductivity of Methane Hydrate. *J. Phys. Chem. B* **2008**, *112* (33), 10207−10216.
(22) Khurana, M.; Yin, Z.; Linga, P. A Review of Clathrate Hydrate Nucleation. *ACS Sustainable Chem. Eng.* **2017**, *5* (12), 11176−11203.
(23) Maddah, M.; Maddah, M.; Peyvandi, K. Molecular dynamics simulation of methane hydrate formation in presence and absence of amino acid inhibitors. *J. Mol. Liq.* **2018**, *269*, 721−732.
(24) Moon, C.; Taylor, P. C.; Rodger, P. M. Molecular Dynamics Study of Gas Hydrate Formation. *J. Am. Chem. Soc.* **2003**, *125* (16), 4706−4707.
(25) Myshakin, E. M.; Jiang, H.; Warzinski, R. P.; Jordan, K. D. Molecular Dynamics Simulations of Methane Hydrate Decomposition. *J. Phys. Chem. A* **2009**, *113* (10), 1913−1921.
(26) Walsh, M. R.; Carolyn, A.; Sloan, E. D.; Amadeu, K.; David, T. Microsecond Simulations of Spontaneous Methane Hydrate Nucleation and Growth. *Science* **2009**, *326* (5956), 1095−1098.
(27) Xu, P.; Lang, X.; Fan, S.; Wang, Y.; Chen, J. Molecular Dynamics Simulation of Methane Hydrate Growth in the Presence of the Natural Product Pectin. *J. Phys. Chem. C* **2016**, *120* (10), 5392−5397.
(28) Zhang, Z.; Walsh, M. R.; Guo, G.-J. Microcanonical molecular simulations of methane hydrate nucleation and growth: evidence that direct nucleation to sI hydrate is among the multiple nucleation pathways. *Phys. Chem. Chem. Phys.* **2015**, *17* (14), 8870−8876.
(29) Sarupria, S.; Debenedetti, P. G. Molecular Dynamics Study of Carbon Dioxide Hydrate Dissociation. *J. Phys. Chem. A* **2011**, *115* (23), 6102−6111.
(30) Abascal, J. L. F.; Sanz, E.; García Fernández, R.; Vega, C. A potential model for the study of ices and amorphous water: TIP4P/Ice. *J. Chem. Phys.* **2005**, *122* (23), No. 234511.
(31) Potoff, J. J.; Siepmann, J. I. Vapor−liquid equilibria of mixtures containing alkanes, carbon dioxide, and nitrogen. *AIChE J.* **2001**, *47* (7), 1676−1682.
(32) Fernández, R. G.; Abascal, J. L. F.; Vega, C. The melting point of ice Ih for common water models calculated from direct coexistence of the solid-liquid interface. *J. Chem. Phys.* **2006**, *124* (14), No. 144506, DOI: 10.1063/1.2183308.
(33) Tung, Y.-T.; Chen, L.-J.; Chen, Y.-P.; Lin, S.-T. Growth of Structure I Carbon Dioxide Hydrate from Molecular Dynamics Simulations. *J. Phys. Chem. C* **2011**, *115* (15), 7504−7515.
(34) Horn, H. W.; Swope, W. C.; Pitera, J. W.; Madura, J. D.; Dick, T. J.; Hura, G. L.; Head-Gordon, T. Development of an improved four-site water model for biomolecular simulations: TIP4P-Ew. *J. Chem. Phys.* **2004**, *120* (20), 9665−9678.
(35) Harris, J. G.; Yung, K. H. Carbon Dioxide's Liquid-Vapor Coexistence Curve And Critical Properties as Predicted by a Simple Molecular Model. *J. Phys. Chem. A* **1995**, *99* (31), 12021−12024.
(36) Sun, R.; Duan, Z. Prediction of CH_4 and CO_2 hydrate phase equilibrium and cage occupancy from *ab initio* intermolecular potentials. *Geochim. Cosmochim. Acta* **2005**, *69* (18), 4411−4424.
(37) Míguez, J. M.; Conde, M. M.; Torre, J.-P.; Blas, F. J.; Pineiro, M. M.; Vega, C. Molecular dynamics simulation of CO_2 hydrates: Prediction of three phase coexistence line. *J. Chem. Phys.* **2015**, *142* (12), No. 124505, DOI: 10.1063/1.4916119.
(38) Abascal, J. L. F.; Vega, C. A general purpose model for the condensed phases of water: TIP4P/2005. *J. Chem. Phys.* **2005**, *123* (23), No. 234505, DOI: 10.1063/1.2121687.
(39) Costandy, J.; Michalis, V. K.; Tsimpanogiannis, I. N.; Stubos, A. K.; Economou, I. G. The role of intermolecular interactions in the prediction of the phase equilibria of carbon dioxide hydrates. *J. Chem. Phys.* **2015**, *143* (9), No. 094506.
(40) Izadi, S.; Anandakrishnan, R.; Onufriev, A. V. Building Water Models: A Different Approach. *J. Phys. Chem. Lett.* **2014**, *5* (21), 3863−3871.
(41) Xiong, Y.; Shabane, P. S.; Onufriev, A. V. Melting Points of OPC and OPC3 Water Models. *ACS Omega* **2020**, *5* (39), 25087−25094.
(42) McMullan, R. K.; Jeffrey, G. A. Polyhedral Clathrate Hydrates. IX. Structure of Ethylene Oxide Hydrate. *J. Chem. Phys.* **1965**, *42* (8), 2725−2732.
(43) Takeuchi, F.; Hiratsuka, M.; Ohmura, R.; Alavi, S.; Sum, A. K.; Yasuoka, K. Water proton configurations in structures I, II, and H clathrate hydrate unit cells. *J. Chem. Phys.* **2013**, *138*, No. 124504.
(44) Abraham, M. J.; Murtola, T.; Schulz, R.; Pall, S.; Smith, J. C.; Hess, B.; Lindahl, E. GROMACS: High performance molecular simulations through multi-level parallelism from laptops to supercomputers. *SoftwareX* **2015**, *1−2*, 19−25.
(45) Van Der Spoel, D.; Lindahl, E.; Hess, B.; Groenhof, G.; Mark, A. E.; Berendsen, H. J. GROMACS: Fast, flexible, and free. *J. Comput. Chem.* **2005**, *26* (16), 1701−1718.
(46) Essmann, U.; Perera, L.; Berkowitz, M. L.; Darden, T.; Lee, H.; Pedersen, L. G. A smooth particle mesh Ewald method. *J. Chem. Phys.* **1995**, *103* (19), 8577−8593.
(47) He, Z.; Linga, P.; Jiang, J. What are the key factors governing the nucleation of CO_2 hydrate? *Phys. Chem. Chem. Phys.* **2017**, *19*, 15657−15661.
(48) Duan, Z.; Sun, R.; Zhu, C.; Chou, I. M. An improved model for the calculation of CO2 solubility in aqueous solutions containing Na^+, K^+, Ca^{2+}, Mg^{2+}, Cl^-, and SO_4^{2-}. *Mar. Chem.* **2006**, *98* (2), 131−139.

https://doi.org/10.1021/acsomega.3c05673
ACS Omega 2023, 8, 39847−39854